Recurrence spectroscopy of potassium near ionization using laser diodes

M. L. Keeler

Department of Physics, University of Minnesota–Morris, Morris, Minnesota 56267, USA

In this investigation recurrence spectra of potassium are acquired using 405 and 980 nm laser diodes. Atoms were excited to Rydberg-Stark states ($n \approx 70$) resonantly via the $5p_{3/2}$ state and recurrence spectra were obtained near the classical ionization threshold. The data suggest that the outgoing distribution of electrons is more symmetric in potassium than in hydrogen or sodium and that phase shifts incurred by the electron wave function as it passes through the atomic core cause regular destructive interference within the recurrence spectra.

Recurrence spectroscopy is a means of extracting a semiclassical action spectrum from the absorption spectra of Rydberg states in the presence of an external field. A recurrence spectrum can be obtained by taking the Fourier transform of a scaled absorption spectrum. The scaled absorption spectrum, a taken along of constant scaled energy, $\varepsilon = EF^{-1/2}$, is experimentally obtained by advancing the excitation energy (E) while keeping ε constant (where F is the external electric field strength). Since the development of the semiclassical theory known as *closed orbit theory*, there have been experimental investigations of hydrogen [1], helium [2–5], lithium [6,7], argon [8], xenon, sodium [9,10], strontium [11,12], and most recently barium and calcium [13]. Only limited amounts of data in the lithium, helium and sodium studies have included data above the classical ionization threshold ($\varepsilon = -2$). This study reports the recurrence spectra of potassium, taken in the vicinity of the ionization threshold. A two-photon resonant transition involves a blue laser diode to excite the valence electron to an intermediate $5p$ state, then a second infrared laser to populate Rydberg states.

Infrared and ultraviolet beams are sent counterpropagating through a chamber containing a set of Stark plates. Based on the vapor pressure of potassium and the temperature of the source, the background pressure of potassium within the interaction region is below 5 mtorr. The Stark plates also serve as the detector, with the top plate held at a negative voltage. The two laser beams excite potassium vapor into Rydberg states that are quickly ionized from collisions with the background gas. Under dc Stark-field conditions the electrons are accelerated to the anode (bottom plate) and sent to a simple current to voltage converter (2.4×10^6 A/V). The mean free path for a free electron to ionize background neutral atoms is on the order of a few cm; thus signal gain from cascading ionization is small. Secondary emission produced by potassium ions hitting the top plate is also negligible. Signal at $n = 30$ is still very strong with fields as low as 0.016 v/cm, essentially field-free spectra, suggesting that collisional ionization is efficient as a detection mechanism over the principle quantum number regime investigated, $n = 67$–71. Rydberg production is modulated via an optical chopping wheel and a lock-in amplifier detects the corresponding modulated signal current.

Since the introduction of the blue laser diode by the Nichia Corporation in 1999 very few spectroscopic investigations in atomic physics have utilized this option. This is pri-

marily due to their limited tuning range which restricts their uses to a handful of atomic transitions, one of which is the $4s$ ground state to the $5p$ excited state of potassium [14]. The Sanyo 5 mW laser diode (model DL-3146-151) has a chosen manufactured wavelength of 405 nm and happens to be close to the ground-state $4s\ ^2S_{1/2} \rightarrow 5p\ ^3P_{3/2,1/2}$ excited state transitions, 404.5 and 404.8 nm, respectively. The laser diode can be tuned to either transition in the traditional way, using temperature control and/or optical feedback. One practical concern when considering UV or blue laser diodes for spectroscopic use is that they demonstrate less temperature tunability than traditional visible or IR laser diodes, approximately 0.04 nm/°C versus 0.2 nm/°C, respectively [15].

The mount for the 405 nm laser allows for both temperature control and grating feedback [16–18]. Utilizing a beam splitter within the Littrow cavity provides good feedback and allows for the adjustment of the grating angle without influencing the final beam alignment. A piezoelectric element is incorporated into the optical mount of the diffraction grating for fine-tuning of the grating angle. Modes associated with the spacing of the optical elements can adversely affect the output of the laser, so a second PZT element, is used to move the grating closer or further from the beam splitter without adjusting the grating angle. With this arrangement approximately 3 mW of laser power is available for the experiment. The tuning of the laser diode is accomplished by monitoring fluorescence associated with the $5p$ state directly from the experimental chamber using a CCD camera.

Once a population of excited $5p$ atoms is established, a second laser diode operating near 980 nm can excite to Rydberg states. The wavelength of this laser is continuously scanned in a semipassive manner by allowing the temperature to rise at a rate of 0.005 °C/s. During a scan the wavelength is continuously monitored by a vacuum-spaced etalon and wavemeter (the design is a modified version of the description in Fox *et al.* [19]). Figure 1 shows an example scan including wavemeter data (with linear fit), etalon, and Rydberg signals as a function of time. The scan range is typically limited to less than $\frac{1}{2}$ nm by laser diode mode hops.

Recurrence spectroscopy is a means of obtaining excited spectra in such a way as to allow for a direct semiclassical analysis and dynamical interpretation. The ideas and concepts behind recurrence spectroscopy are beyond the scope of this Brief Report and more details can be found elsewhere
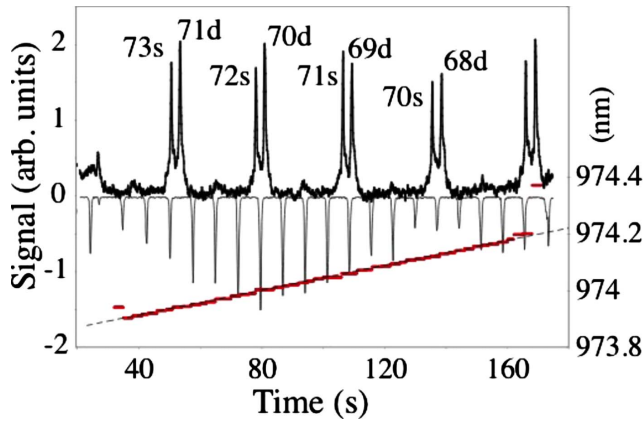
FIG. 1. (Color online) Plot of wavemeter (gray dots, lower half of plot), etalon signal (inverted thin line), and Rydberg signal (dark line) as a function of time. Signal levels are in arbitrary units on left side scale; wavemeter values are on right side scale. The thin dotted line represents a linear fit to wavemeter data. The detected signal spans the Rydberg range $n=68-71$.

[1–13]. The x axis of a recurrence spectrum is typically the scaled action ($\widetilde{S}$), and is related to the classical action of the trajectory. The recurrence strength is a *semiclassical* approximation and is determined not only by the classical stability of well defined orbits, but also by the quantum mechanics in the vicinity of the nucleus. In the semiclassical approximation, all classical orbits are launched simultaneously with the distribution of launching angles being determined by the initial quantum state and laser polarization. Within the final recurrence spectra this probability distribution is mathematically incorporated into the final measured distribution of classical orbit probabilities. In addition, as classical orbits return to the core they are capable of interfering with one another. Finally, the returning electron wavefront experiences diffraction as it passes by the core [20]. The latter two influences have been noted by several groups and are critical to interpreting experimentally obtained recurrence spectra, particularly at low quantum numbers ($n=20-30$) [21].

Experimentally, to maintain a constant scaled energy, the Stark field must be updated in real time as the laser wavelength is being scanned. Rather than perform real-time measurements and update the field accordingly, a reference scan is obtained under field free conditions, and a program of Stark-voltage with respect to time is pre-determined. By far the largest uncertainty in the scaled energy comes from the knowledge of the Stark field, and in this experiment limits the uncertainty to $\Delta\varepsilon=\pm0.07$ at $\varepsilon=-2$. The range of the absorption spectrum scanned, limited by the mode-hops of the diode laser, restricts the final resolution in scaled action. For this investigation, the absorption spectrum covers a range of approximately five Stark manifolds, and this limits the resolution in scaled energy to approximately $\Delta\widetilde{S}\approx0.1$. Finally, to simplify orbit identification the scaled action ($\widetilde{S}$) for each recurrence spectrum of Fig. 2 has been multiplied by a factor of $\sqrt{-2\varepsilon}$. This stretch causes all orbits with a constant period ratio (motion along u and v hyperbolic coordinates) to lie on approximately vertical lines [10]. To avoid
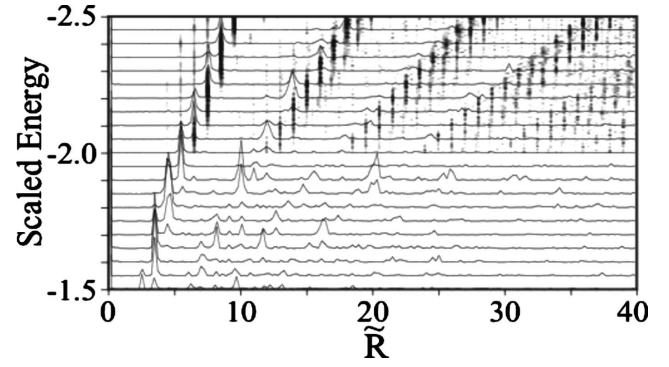
FIG. 2. Experimental recurrence spectra ($n=68.75-73$) are represented as line graphs, offset according to their scaled energies (left scale). For the scaled energy range $\varepsilon=-2.0$ to $\varepsilon=-2.5$ the data is directly compared with a hydrogen computation ($m=0$; $p\to s$ transition; $n=52.75-57$).

using the term "scaled-scaled action" I will refer to this stretched scale as the scaled ratio $\widetilde{R}$. To make experimental peaks more apparent at higher $\widetilde{R}$, the recurrence strength at a given location has been scaled by $\widetilde{R}$.

In order to facilitate integrating the equations of motion, the classical paths of bound electrons in a Stark field are generally computed in semiparabolic coordinates. In which case the orbit shape can be described in terms of the period ratio in the semiparabolic u and v coordinates (t_u/t_v). As noted in previous publications [22,23] orbits organize along bands, with the first band representing orbits with a period ratio, $i/(i+1)$, the second band $i/(i+2)$, and so on. These bands merge and have significant overlap as the external field strength increases and the scaled energy passes $\varepsilon=-2$. A full quantum computation of hydrogen [24], assuming a $p\to s$ transition, was performed to compare directly with the experimental results (see Fig. 2). Despite assumptions in the excitation scheme, the two recurrence spectra show qualitative agreement.

Some differences and similarities found between the hydrogen and potassium recurrence spectra can be attributed to the influence of the quantum defects on oscillator strength. In hydrogen, the probability of exciting from a $p\to d$ state, based on computations of the square of the dipole moment, is larger than exciting a $p\to s$ transition. In contrast, the quantum defects in potassium ($\mu_0=2.18$, $\mu_1=1.714$, $\mu_2=0.277$) reverse this trend, making $p\to s$ transitions significantly more probable than $p\to d$ transitions. This initially explains the similarity between the experimental recurrence spectra and the computed hydrogen $m=0$, $p\to s$ recurrence map.

From the perspective of semiclassical closed orbit theory, the recurrence spectrum reflects the classical dynamics of the excited electron, but also includes the initial launching distribution, orbit interference and the potential for core scattering. The excitation scheme used on potassium in this experiment is similar to those used in investigations of sodium [10,25]. The electron, initially in the $4s_{1/2}$ state is excited, with a UV-photon polarized parallel to the Stark field, to the intermediate $5p_{3/2}$, $m_j=1/2$ state. The second laser, also polarized parallel to the external field, prepares a mixture of
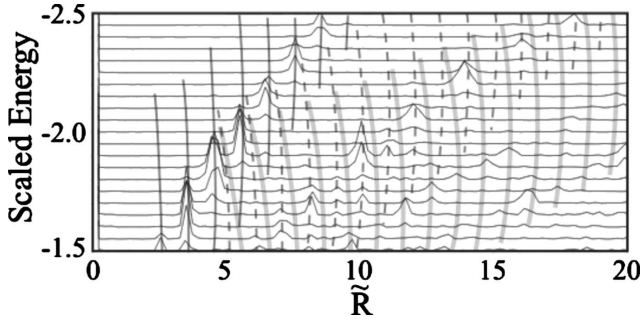
FIG. 3. Experimental recurrence map with locations of classical orbits indicated by lines [$i/(i+1)$ orbits=solid dark line; $i/(i+2)$ orbits=dotted lines; $i/(i+3)$ orbits=thick gray lines].

$m_1 = 0$, 1 Stark manifolds. An expression for the initial angular distribution of electrons was given for the intermediate $3p_{3/2}$, $m_j = 1/2$ state of sodium in Gao *et al.* [26], specifically Eqs. (5.17a) and (5.17b) of this reference. This equation can be written to express the initial angular distribution in potassium.

$$y_0(\theta) = \sqrt{\frac{2}{3}} \sqrt{\frac{1}{3}} I_K(5,1,0) Y_{00}(\theta,0) e^{i\delta_0}$$
$$+ \sqrt{\frac{2}{3}} \sqrt{\frac{4}{15}} I_K(5,1,2) Y_{20}(\theta,0) e^{i\delta_2}, \quad (1a)$$

$$y_1(\theta) = \sqrt{\frac{1}{3}} \sqrt{\frac{1}{15}} I_K(5,1,2) Y_{21}(\theta,0) e^{i\delta_2}. \quad (1b)$$

The final angular distribution $y(\theta)$ is a coherent mixture of $m=0$ and $m=1$ states, with angular distributions described by Eqs. (1a) and (1b), respectively. The phase of the individual components is related to the quantum defects, where $\delta_l = (\mu_l+)(\mathrm{mod}\ 1)\text{-}1/2$. In expression (1a), the uniqueness of the angular distribution is primarily determined by the probability of exciting into the continuum, or ionizing,

$$I(n,l,l') = \sqrt{8} \int_0^\infty R_{n,l}(r) R_{\infty,l'}^{\mathrm{reg}}(r) r^3 dr. \quad (2)$$

For sodium the ratio $I_{\mathrm{Na}}(3,1,0)/I_{\mathrm{Na}}(3,1,2)=0.57$, for hydrogen $I_{\mathrm{H}}(5,1,0)/I_{\mathrm{H}}(5,1,2)=0.41$, while for potassium $I_K(5,1,0)/I_K(5,1,2)=5.63$, indicating that the initial outgoing distribution is significantly more symmetric in potassium than in either hydrogen or sodium.

To positively identify recurrences with specific closed orbits, classical actions were calculated. Figure 3 shows the same experimental recurrence data as Fig. 2 with the expected locations of classical orbits indicated as lines, where the lines extend from the classical uphill bifurcation to the classical downhill bifurcation. The recurrence peaks of the first band lie on orbits with period ratio $i/(i+1)$. The highest *classical* orbit stability occurs near the bifurcations (ends of the lines indicating classical orbits), where the initial launching angle is either parallel or anti-parallel to the external

field. Ignoring the possibility of interference, the final measured orbit probability (recurrence strength) along a line of constant period ratio should be proportional to the classical stability multiplied by the initial launching distribution. Because the initial angular distribution in potassium has more *s* character than *d* we expect significant recurrence strength to be located close to the center of the orbit profile. The peak recurrence strength in potassium lies even closer to the center of the classical orbit range than the distribution calculated for hydrogen, and is consistent with, but not completely explained by, an initially symmetric angular distribution.

Previous studies [6,22,27] note and observe that a non-hydrogenic core can lead to the creation of combination orbits whose action is the sum of two or more hydrogenic orbits. These combination orbits can be interpreted as an electron, in one orbit, scattering classically into a second orbit before returning to the core [28]. In many cases the combination orbits are composed of primitive orbits and their repetitions. While the experimental resolution is low, if combination orbits involving primitive repetitions were strong they should be resolvable, particularly at low field strengths (near $\varepsilon = -2.5$) between the regions of the first and second band ($10 < \tilde{R} < 15$). No such orbits are observed. In addition, the primitive orbits and their repetitions, typically observed at low integer values of $\tilde{R}$, are immeasurably weak. Despite the lack of direct evidence for scattered combination orbits, interference between classical orbits as they return to the atomic core must contribute to the comparative differences between the computed and experimental recurrence spectra shown in Fig. 2.

The orbits in the second band (identified by dotted lines in Fig. 3), particularly below the classical threshold for ionization ($\varepsilon = -2.0$ to -2.5) appear to alternate in recurrence strength. This same effect has been previously noted in both sodium and helium [10,22]. Orbits in this band that occur at integer $\tilde{R}$ values are significantly diminished in strength. These orbits are repetitions of orbits from the first band (for example, the $10/12$ period ratio orbit is a repetition of the $5/6$ orbit) and pass through the nonhydrogenic core twice, in contrast with their immediate neighbors at half-integer values of $\tilde{R}$ which only encounter the non-hydrogenic core once. From a semiclassical perspective, the additional travel through the shielded core introduces a phase shift ϕ [Eqs. (7.14a) and (7.14b) of Ref. [27]] to the classical path where $\phi \approx 2\delta_l - \pi$. A phase shift in itself will not produce any measurable interference effects. Other core-scattered orbits, unresolved in action from the expected hydrogenic orbits, provide a background for this regular modulation of phase to interfere with. Despite the fact that the recurrence strength is a coherent sum of many unresolved orbits, the primary contributors to the second band of recurrence strengths are still the $i/i+2$ orbits, and these experience a regular modulation in phase according to the number of interactions with the electronic core.

As the external field goes beyond the classical threshold for ionization ($\varepsilon > -2$) the uphill-oriented orbits which have not ionized become shorter in length (action) and are found at increasingly lower values of $\tilde{R}$. Just above the classical ionization threshold, peaks in the first band, particularly the

4/5 peak (located near $\widetilde{R}$=4.5) and the 5/6 peak (located near $\widetilde{R}$=5.5) appear significantly stronger than neighboring peaks. The lines indicating classical trajectories in Fig. 3 suggest that the recurrence strengths associated with the 4/5 and 5/6 orbits are enhanced where the downhill oriented 4/5, 4/6, 4/7; and 5/6, 5/7, 5/8 period ratio orbits converge. A similar mechanism may play a role in enhancing recurrence strengths in other bands. At high field strengths, $\varepsilon > -1.75$, the band structures which are distinct for moderate fields become thoroughly intermixed. At these scaled energies the density of orbits increases such that each recurrence peak is an unresolved coherent sum of classical orbits. To distinctly resolve these would require tuning over a larger energy range than is possible with the infrared diode currently in use.

The application of blue laser diodes in a two-photon resonant excitation of potassium into highly excited Rydberg states was demonstrated. Recurrence spectroscopy was achieved by tuning an external electric field simultaneously with the second IR laser. In comparison with calculated hydrogen recurrence spectra, the experimental potassium data shows recurrence strength shifted away from classical bifurcation points. This is consistent with, but not entirely explained by, semiclassical expressions for the initial launching distributions of electrons from the atomic core. The experimental data also shows a modulation in recurrence strength along the second band of orbits, with orbits that pass through the core twice experiencing a phase shift that causes them to diminish in strength when interfering with other nonhydrogenic orbits.

[1] S. Freund, R. Ubert, E. Flothmann, K. Welge, D. M. Wang, and J. B. Delos, Phys. Rev. A **65**, 053408 (2002).

[2] D. Wang and S. Ding, Phys. Rev. A **68**, 023405 (2003).

[3] A. Kips, W. Vassen, and W. Hogervorst, Phys. Rev. A **59**, 2948 (1999).

[4] A. Kips, W. Vassen, W. Hogervorst, and P. A. Dando, Phys. Rev. A **58**, 3043 (1998).

[5] M. L. Keeler and T. J. Morgan, Phys. Rev. A **59**, 4559 (1999).

[6] M. Courtney, N. Spellmeyer, H. Jiao, and D. Kleppner, Phys. Rev. A **51**, 3604 (1995).

[7] M. Courtney, H. Jiao, N. Spellmeyer, and D. Kleppner, Phys. Rev. Lett. **73**, 1340 (1994).

[8] M. L. Keeler, H. Flores-Rueda, J. D. Wright, and T. J. Morgan, J. Phys. B **37**, 809 (2004).

[9] U. Eichmann, K. Richter, D. Wintgen, and W. Sandner, Phys. Rev. Lett. **61**, 2438 (1988).

[10] S. N. Pisharody, J. G. Zeibel, and R. R. Jones, Phys. Rev. A **61**, 063405 (2000).

[11] X. J. Liu, J. W. Cao, M. S. Zhan, and J. Connerade, J. Phys. B **35**, 2069 (2002).

[12] M. S. Zhan, X. J. Liu, J. W. Cao, and J. Connerade, J. Phys. B **34**, 1175 (2002).

[13] J. Murray-Krezan, J. Kelly, M. R. Kutteruf, and R. R. Jones, Phys. Rev. A **75**, 013401 (2007).

[14] U. Gustafsson, J. Alnis, and S. Svanberg, Am. J. Phys. **68**, 660 (2000).

[15] C. Eichler, Annual Report, Optoelectronics Dept., University of Ulm, Germany, 2001 (unpublished).

[16] K. B. MacAdam, A. Steinbach, and C. Wieman, Am. J. Phys. **60**, 1098 (1992).

[17] C. J. Hawthorn, K. P. Weber, and R. E. Scholten, Rev. Sci. Instrum. **72**, 4477 (2001).

[18] V. V. Vassiliev, S. A. Zibrov, and V. L. Velichansky, Rev. Sci. Instrum. **77**, 013102 (2006).

[19] P. J. Fox, R. E. Scholten, M. R. Walkiewicz, and R. E. Drullinger, Am. J. Phys. **67**, 625 (1999).

[20] J. Gao and J. B. Delos, Phys. Rev. A **56**, 356 (1997).

[21] M. L. Keeler, H. Flores-Rueda, T. J. Morgan, and J. Shaw, Phys. Rev. A **69**, 012103 (2004).

[22] M. Keeler and T. J. Morgan, Phys. Rev. Lett. **80**, 5726 (1998).

[23] J. Main, G. Wiebusch, K. Welge, J. Shaw, and J. B. Delos, Phys. Rev. A **49**, 847 (1994).

[24] M. L. Keeler, Phys. Rev. A **76**, 052510 (2007).

[25] J. Gao, J. B. Delos, and M. Baruch, Phys. Rev. A **46**, 1449 (1992).

[26] J. Gao and J. B. Delos, Phys. Rev. A **46**, 1455 (1992).

[27] P. A. Dando, T. S. Monteiro, D. Delande, and K. T. Taylor, Phys. Rev. A **54**, 127 (1996).

[28] B. Hupper, J. Main, and G. Wunner, Phys. Rev. A **53**, 744 (1996).